Measuring Visual Threshold of Inkjet Banding

Chengwu Cui, Dingcai Cao and Shaun Love
Lexmark International, Inc.
740 New Circle Road, Lexington, KY40550

Abstract

Banding can be a major defect in inkjet printing. Knowing the visual sensitivity threshold of inkjet banding is therefore useful for understanding and pushing the technological limit of inkjet printing. There are many reports on the measurement of the human contrast sensitivity using self-luminous sinusoidal contrast targets. There are also reports on measuring the contrast sensitivity of sinusoidal banding on hardcopy targets. However, there has been no report on measuring visual threshold of banding defects that are characteristic of inkjet printing, which is usually not sinusoidal, despite the evidence that the visual threshold of a complex pattern may not be able to be predicted based on each of its harmonic components. In this paper, we report a study on measuring the human visual threshold of real-life inkjet banding defects. Inkjet banding samples were produced by simulating a type of actual inkjet print banding with a high quality proofing system. We simulated bandings at five different frequencies and various contrast levels and at a gray level corresponding to 25% pixel coverage. Fifty observers participated in a visibility and objectionability test with no restriction to view distances under normal office lighting condition and under special lighting for critical proofing viewing. The results obtained show lower threshold values in comparison to reported results on sinusoidal bandings.

Introduction

Swath-by-swath colorant deposition on media by an inkjet printing system makes print head defects and other system errors to show periodically across the page, forming the so-called banding defect. Inkjet banding defects are characteristically different from banding defects produced by other printing technologies such as electro-photographic printing. In addition to some high frequency noise, the banding defects of an inkjet system generally appear to have sharp edges of square waves. This distinctive banding pattern can be highly objectionable on a smooth tone region of an image, such as a human face. Once regarded as a defect, the human visual system can detect the banding pattern with remarkable sensitivity.

If we define the contrast as the ratio of the difference of the peak and valley to the sum of the peak and valley of the waveform, we can compare the visual effects of a square wave pattern and a sine wave pattern. Fig. 1 (a) and (b) show banding patterns formed by the two wave patterns, respectively. If the two patterns were to appear over a portrait image, the difference can be more obvious as demonstrated in Fig. 2 (a) and (b).

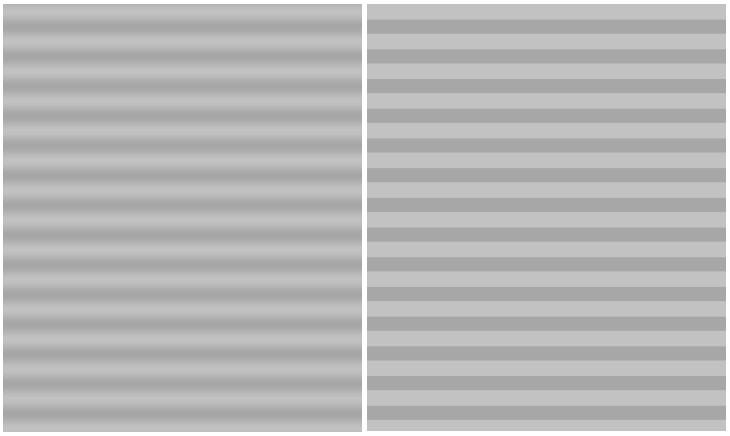

(a) (b)

Fig. 1 Comparison of the banding pattern of a sine wave and a square wave of the same frequency and contrast over a flat field image. (a) sine wave; (b) square wave.

Mathematical transformation such as the Fourier analysis has often been used to analyze periodic signals. The Fourier analysis decomposes a periodical signal, such as a square wave banding pattern, into sine waves of various frequencies. For a square wave of amplitude of one and period w as a function of x, it can be represented by the following infinite series,

$$\frac{4}{\pi}\left[\sin\frac{2\pi x}{\omega}+\frac{1}{3}\sin 3\frac{2\pi x}{\omega}+\frac{1}{5}\sin 5\frac{2\pi x}{\omega}+\frac{1}{7}\sin 7\frac{2\pi x}{\omega}+\ldots\right] \qquad (1)$$

Fig 3 shows the decomposition of the square wave into various sine waves by the Fourier series (up to the 7th harmonic shown).

(a) (b)

Fig. 2 Comparison of the banding pattern of a sine wave and that of a square wave of the same frequency and contrast over a portrait image. (a) Sine wave; (b) square wave.

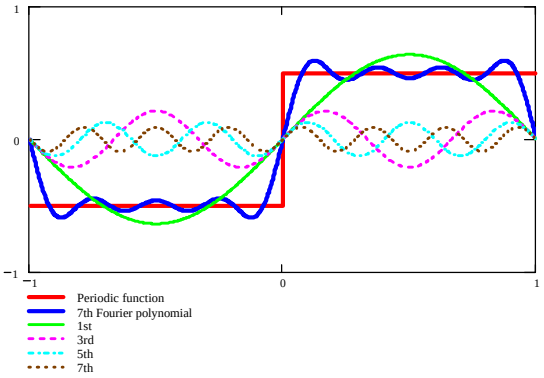

Fig. 3. The square wave, its representation with a 7^{th} order Fourier polynomial, and its 1^{st}, 3^{rd}, 5^{th} and 7^{th} harmonics.

The sine waves can pass through a linear system with modified amplitude and phase while maintaining its original waveform. Such a linear system can therefore be characterized by its capability of passing the sine waves of various frequencies. The modulation transfer function (MTF) is often used to describe such capability. The Fourier method has been successfully applied to optical systems and the optical portion of the visual system are often treated accordingly. In its clinical application, the inverse of the visual contrast threshold as a function of spatial frequency is often called the visual contrast sensitivity function. It describes the limit of the visual system as a whole, both optical and neurological. The corresponding modulation transfer function is often called the visual transfer function of the visual system. In printing quality analysis, the banding defect is often assessed against the visual transfer function of the visual system.

Can we predict the visual sensitivity threshold for a square wave banding pattern from that of a sine wave? Because the higher harmonics of a square wave have amplitudes of 1/3, 1/5, …, times of that of the fundamental harmonic, respectively, it might be expected that the higher harmonics should be below the visual threshold and therefore not visible at relative higher spatial frequencies. Because the amplitude of fundamental harmonic is about 1.27 times that of the sine wave of the same contrast, the sensitivity threshold of a square wave should be 1/1.27 of that of the sine wave. Indeed, this was proven by Campbell and Robson (1967) under stringent test conditions and controls to the variations of the optical portion of the visual system. However, they also found, under their conditions, there were large discrepancies for spatial frequencies under 0.8 cycle/degree. They found that they only could explain the results if they assumed that there were separate visual sensitivity functions, each tuned to a specific spatial frequency. This finding shows that one cannot use one overall visual transfer function to evaluate complex patterns at the lower spatial frequencies. In other words, the visual sensitivity threshold to square wave banding cannot be derived by decomposing it into sine waves and filtering by the visual transfer function at these low spatial frequencies. Inkjet banding spatial frequency is related to the dimension of the nozzle array and the number of passes used for a specific printing mode. Common banding frequencies range approximately from 1 to 20 cycles/inch (cpi). Because prints are viewed at the normal viewing distance (~12 inch), such a range corresponds to very low frequency end of the visual transfer function (~ 0.2-4 cycle/degree) .

Even if a single visual transfer function could be applied, it must be pointed out that potential optical variations of the visual system under different test conditions and for a relatively small number of observers may produce large errors when used for general banding pattern defect evaluations. Most published results also used luminous displays to generate the target stimuli. The difference between reflective targets and self-luminance targets cannot be ignored. Burningham and Bouk (1994) measured threshold visibility and objectionability of sinusoidal banding in reflection prints to verify data based on luminous display reported by Van Nes and Bouman (1967). Based on their product specification development experience, they felt that the often-quoted visual transfer function might be too tight. Their results confirmed that suspicion. Although the spatial frequency range of interest to their study is different from ours here, the concern for reflective stimuli is justified. The optical portion of the

visual system can change its characteristics and performance significantly for different viewing conditions and stimuli. The pupil size, state of accommodation, and ambient stray light can make significant contributions to the final modulation transferring property of the visual system. All these could be contributors for the large discrepancies found by Burningham and Bouk. For square wave patterns, the sharp edges may provide much stronger stimuli for ocular accommodation, which is essential for viewing near distance target.

In summary, all these potential variables make it difficult to evaluate inkjet banding defects by applying a universal visual transfer function that might have been obtained for other vision research and application purposes. On the other hand, from the perspective of applied science, we can devise a measurement to simulate real print viewing conditions and real print targets to measure the visual inkjet banding thresholds for a relative large number of observers. The results should be directly applicable to inkjet banding assessment. Along this direction, we conducted a measurement of the visual sensitivity threshold of a typical inkjet banding pattern over a flat field image at various typical spatial frequencies under normal viewing conditions.

Experiment

Sample preparation

A Polaroid PolaProof™ 1420 system was used to produce print samples of typical inkjet bandings defects over a flat field image. The printing system was a binary printing system with a spatial resolution of 2400 dpi. In order to achieve threshold contrast levels while avoiding halftone artifacts, it was determined that a 24x24 halftone cell size had to be used. The banding profile was extracted from a typical inkjet-banding pattern as shown in Fig. 4 (a). Fig. 4 (b) shows a typical image with simulated banding given by the banding profile used.

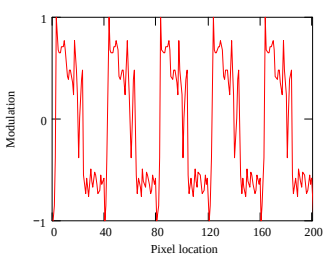

(a)

(b)

Fig.4. (a) Inkjet banding profile used to simulate banding defects; (b) an image with the simulated banding using the banding profile shown in (a).

The spatial frequencies, characteristic of inkjet banding, were 2, 4, 8, 16, and 32 cycles per inch (cpi). The average density level in each image was set according to an approximately 25% pixel coverage, a known defect-sensitive density level. At each spatial frequency, 15 contrast levels were used and they were intended to cover a range from sub-threshold banding to highly visible banding. The contrast values of the simulated banding were determined by correlating image pixel intensity values used in the simulation with measured CIE1976 L* values based on three copies of 180 intensity levels in the interested density range. The samples were 3"x2.5" and mounted on 5"x4" neutral gray cardboards for handling convenience.

Observers

Fifty observers participated in this experiment voluntarily. They were employees at Lexmark International, Inc. with ages ranged from 20-50 years old and of various technical backgrounds.

Test conditions

The test was conducted in a windowless room with walls painted to a neutral gray (N7). Two illumination systems were used. One was a regular office lighting box installed in the ceiling and produced 420 lux illumination on the surface of the test desk. The other system was an 8-lamp GretagMacbeth™ overhead fluorescent daylight D50 luminaire, producing an illumination level of about 1200 lux on the surface of the test desk.

Method

Samples of all spatial frequencies and all contrast levels were randomly mixed into one pile and presented to the observer. The observer was asked to sort the samples into three piles according to the degree of banding defect seen: 1) no banding; 2) with acceptable banding; 3) with unacceptable banding.

The instructions to the observers were:

You will be presented a series of printing samples under two different illuminators. We would like to know whether you see banding, a printing defect, in each sample. Without the banding defect, the sample should be perceptually uniform. If you see banding in a sample, please consider whether the banding is acceptable according to your standard on printing quality. Place the samples that you see no banding on your right side, those with acceptable banding in the middle, and those with unacceptable banding on the left side. Please hold the samples in the direction as indicated and ignore other printing defects.

The observers were instructed to hold the samples in the direction so that banding would be horizontal. To speed up the test, two identical sets of samples were prepared for use under each illumination conditions. The samples were

shuffled randomly before the test for each observer. After the test under one illumination condition was finished, the observer moved to another illumination condition, and rested for 2 minutes to get adapted to the illumination condition. The test lasted for approximately 20 minutes for each observer.

Results

For each sample under a specific illumination, the proportion of observers seeing banding and the proportion of observers seeing unacceptable banding were computed, respectively. Corresponding psychometric functions were constructed, by linearly fitting the z scores of the proportions, to determine the banding visibility thresholds and the banding objectionability thresholds. Typical constructed psychometric functions are shown in Fig. 5 for 2 cpi pattern under critical viewing illumination condition. As can be expected, the visibility psychometric curve is much steeper than the objectionability curve. With a 24x24 halftone dot size, at the lightness level of the image (L* ~70), the modulation resolution the printing system was estimated at about 0.1%, therefore the derived contrast levels may not reflect the true contrast level. Three samples of adjacent nominal contrast levels might have the same true contrast level. In fact, the problem can be seen in Fig.5. Some samples tended to have the "group-effect". In theory, increasing the halftone cell size could result a higher contrast resolution. However, the sample printing system resolution of 2400dpi resulted in a 100 lpi resolution with a 24x24 halftone cell size. A larger halftone cell would have produced unacceptable halftone artifacts. Despite such a limitation in producing the desired contrast level, the psychometric functions obtained as shown in Fig. 5 provided sufficient information to derive the threshold values.

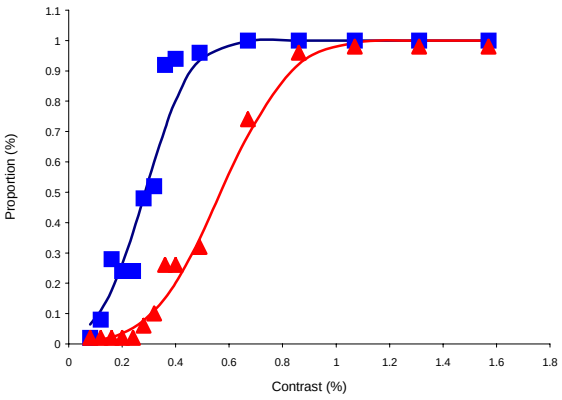

Fig.5. The constructed psychometric function for the 2 cpi pattern under critical viewing illumination condition.

The threshold contrasts of visibility and objectionability were defined at the 50% proportion level. The contrasts at the 25% and the 75% level were also computed. The results were shown in Fig. 6 and 7. For comparison, the visibility threshold for variable viewing distance for flat field and the objectionability threshold for flat field image from Burningham & Bouk's study were adapted into the corresponding figures.

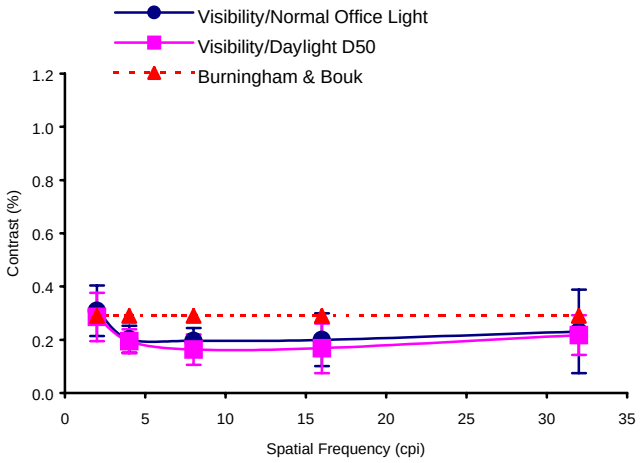

Fig.6. Inkjet banding visibility thresholds under normal office light and critical viewing light, respectively.

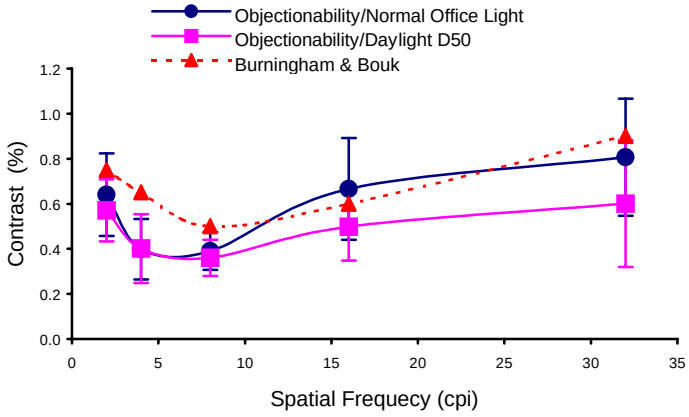

Fig.7. Inkjet banding objectionability thresholds under normal office light and critical viewing light, respectively.

Fig. 6 and 7 show the observers were most sensitive to banding at mid-range spatial frequencies (8 and 16 cpi). At the mid-range spatial frequencies, increased illumination level would also increase the sensitivity.

To show the difference between the visibility threshold and the objectionability threshold, the two thresholds under

critical viewing illumination were shown together in Fig. 8. As can be expected, the objectionability thresholds were substantially higher than the visibility thresholds. The differences were larger at higher spatial frequencies. It indicates that the observers were more tolerant of higher spatial frequency bandings.

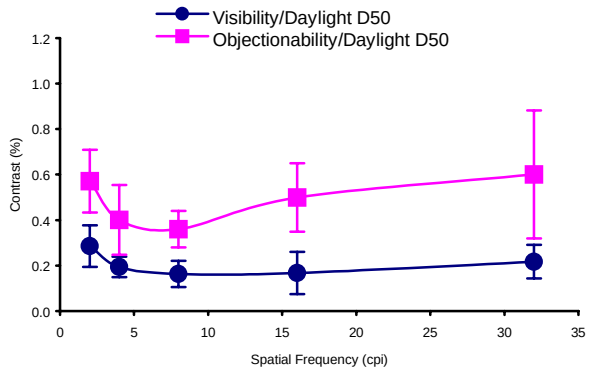

Fig.8. Comparison of the visibility threshold and the objectionability threshold under critical viewing illumination.

There were many other critical differences between Burningham and Bouk's test and our test in addition to the difference in banding profiles. They mentioned an average density level of 0.62, which was dark than the average density used in this study. Their illumination level was also higher than the level used in our test. Their visibility threshold was taken at the 80% level and their objectionability threshold was taken at the 70% level, which should be close to our 75% levels. Despite the many differences between the two measurements, the two results were surprisingly consistent. Our visibility threshold data were significantly lower than Burningham and Bouk's data except at the lowest spatial frequency. At 2cpi, it seemed Burningham and Bouk's threshold was lower than our 75% threshold, which is difficult to explain. Their data showed a surprising constant threshold across a large range of spatial frequencies.. For 4, 8, and 16 cpi, our thresholds were lower as expected for square wave banding patterns. At 32 cpi, the two thresholds were identical. For the objectionability thresholds, the two thresholds were about the same, indicating that the objectionability thresholds for the two types of banding patterns are close.

Discussion

The major challenge for this type of studies was to make the simulation samples of the contrast resolution needed to cover the threshold contrast range and to derive the true modulation contrast. It also raised the question of measuring banding and other printing defects with some measuring devices only capable of outputting 8 bit data.

The visibility thresholds measured here showed that the human visual system is superbly sensitive to inkjet banding patterns. The thresholds can be as low as 0.1% modulation. The thresholds are not uniform across the spatial frequency region of technological interest to inkjet printing. Although the dependence on spatial frequency is not dramatic, it can make a significant difference when rendered in printing quality in the banding defect sensitivity threshold region.

The goal of this study was to measure the thresholds of inkjet print banding defects and we found that the square wave like type of inkjet banding did have lower thresholds than that from reported sine wave bandings. Due to numerous measurement differences, it is difficult to make precise comparisons with reported data. At the lower end spatial frequencies, the threshold does not rise as dramatically as can be expected for sine wave bandings based on the visual transfer function, consistent with Campbell and Robson's finding. Extensions of this work to equivalent sine wave banding patterns and perfect square wave patterns perhaps could bring more insight into how exactly the visual system responds.

The banding profile used in this study does not have a perfect square wave profile. It also consisted of some high frequency banding lines that likely resulted from single nozzle errors. To show how far this banding profile differs from the perfect square wave, Fig. 9 shows the FFT analysis of the pattern against that of a perfect square wave. Because, the contrast was calculated peak to valley, the square wave part of the inkjet banding profile used here had a lower contrast than the perfect square wave. However, the general Fourier spectrums are very similar.

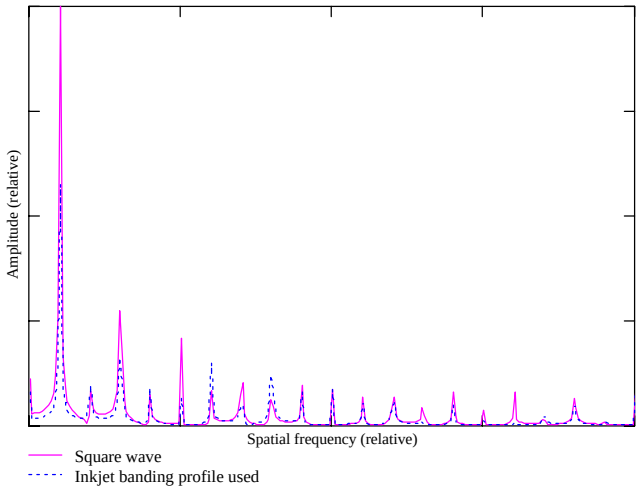

Fig.9. Fourier spectrum of the inkjet banding pattern used in this study and that of the perfect square wave.

This study shows that the observers clearly could tolerate some banding patterns as printing defects. The observers generally can tolerate twice to three times the visibility threshold from low to higher frequencies of interest to inkjet banding defects. Burningham and Bouk found strong dependency of such tolerance on image content, which is beyond what the visual transfer function can explain. Fig. 2. (a) and (b) also show the strong effect indisputably. If we look at the effect of the higher harmonics of Fig. 2 (b), as shown in Fig. 10, the effect is not as striking on the portrait image as on the flat field. The combined effect as shown in Fig. 2(b) is indeed striking, and perhaps requires us to draw on more knowledge of our visual system to explain than merely resorting to the visual transfer function.

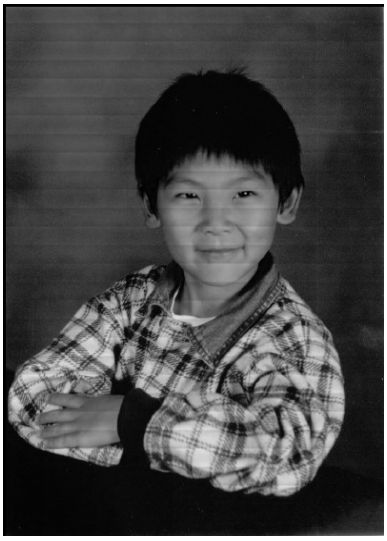

Fig.10. Higher order harmonics of the square wave pattern over a portrait image.

Conclusions

We measured the visibility thresholds of typical inkjet banding patterns under normal print viewing conditions. The obtained thresholds are lower when compared to other measurements using sine wave banding patterns. The data can be used for typical inkjet banding defects evaluation. We also measured the objectionability thresholds for flat field image and found the observers tolerated two to three times the visibility thresholds from 2cpi to 32 cpi. However, the objectionability thresholds should be highly dependent on image content. Our results also showed that the thresholds were lower for strong illumination although the effect virtually vanished for 2 and 4 cpi.

Acknowledgement

We would like to thank our colleagues, Drs. Tomasz Cholewo, Mike Lhamon, and Brian Cooper for helps and or suggestion in making the samples. We are also grateful for the participation of all the observers.

References

1. F. W. Campbell and J. R. Robson, Application of Fourier analysis to the visibility of gratings, J. Physiol., Volo. 197, P551-566, 1968.
2. Normal Burningham and Theodore Bouk, Threshold visibility and objectionability of banding in reflection prints, NIP10, New Orleans, Louisiana, P548-551, 1994.
3. F. Van Nes and M. Bouman, Spatial modulation transfer in the human eye, J. Opt. Soc. Of Am., Vol. 57, N0. 3, 1967.